# epl draft

# Threefold onset of vortex loops in superconductors with a magnetic core

Mauro M. Doria[1,2] [(a)], Antonio R. de C. Romaguera[1,2], M. V. Milošević[1,3] and F. M. Peeters[1]

[1] *Departement Fysica, Universiteit Antwerpen, Groenenborgerlaan 171, B-2020 Antwerpen, Belgium*
[2] *Instituto de Física, Universidade Federal do Rio de Janeiro, C.P. 68528, 21941-972, Rio de Janeiro RJ, Brazil*
[3] *Department of Physics, University of Bath, Claverton Down, BA2 7AY Bath, United Kingdom*

**Abstract.** - A magnetic inclusion inside a superconductor gives rise to a fascinating complex of *vortex loops*. Our calculations, done in the framework of the Ginzburg-Landau theory, reveal that *loops always nucleate in triplets* around the magnetic core. In a mesoscopic superconducting sphere, the final superconducting state is characterized by those confined vortex loops and the ones that eventually spring to the surface of the sphere, evolving into *vortex pairs* piercing through the sample surface.

Examples of one- or multi-dimensional collections of topological defects arise in various physical systems, such as vortices in quantum fluids [1], dislocations in solids [2], global cosmic strings [3, 4], and polymer chains [5]. Changes of symmetry in their structural and dynamical properties often lead to very rich phase transitions. In superconductivity, the structure and symmetry of the vortex lines has been a major issue even in the early days, when Abrikosov [6] proposed a square pattern for the lattice of penetrating flux tubes in bulk superconductors; later on, Kleiner *et al.* [7] found that the most efficient way to pack interacting parallel rods is actually through a hexagonal pattern. However, in systems with reduced dimensionality, the Abrikosov symmetry of the vortex state can be strongly affected by the sample boundaries. In mesoscopic superconductors, where the volume to surface area ratio is small [8], strong lateral confinement may impose the formation of multiquanta ('giant') vortices [9, 10], while the shape of the boundary directs the symmetry of the final vortex configuration [11].

In this Letter, we consider a novel vortex structure that stems from the specific *inhomogeneous* magnetic field of a point like magnetic dipole with moment $\mu$ in the center of a superconducting sphere. This magnet is the only source and sinkhole of vortex lines and sets an axis around which the vortex state exhibits a discrete symmetry. Because the sphere does not break this degeneracy many of the present results also apply for a magnetic inclusion in a bulk superconductor.

Therefore, the present analysis is very different from earlier studies of vortex and antivortex structures in superconductor/magnet hybrids [12–14] where magnetic dots were placed near, but *outside* a *thin* superconducting sample. While in the latter case vortices were two-dimensional (2D) structures characterized by a coin-like core, here they are lines in three-dimensional (3D) space, set on a formalism that comprises the full 3D Ginzburg-Landau theory, thus far more complex than previous works. Consequently, novel vortex phases with profound 3D features are found for these sets of curved vortex lines, made of *confined vortex loops* (**CVL**s) and *external vortex pairs* (**EVP**s).

For small $\mu$, as shown later, we find that the vortex state is made of *exactly three* confined vortex loops around the dipole axis. For an increasing magnetic moment $\mu$ more elaborate vortex arrangements arise because of the inhomogeneity of the field. This threefold growth of vortex loops in our system is shown here to be a consequence of the energetic balance. Threefold symmetry has been a source of inspiration since the sixties when its discovery in hadronic physics has led to quarks as the basic constituents of matter. Recently, experimental evidence was found for the onset of trimer bound states in ultracold gases of caesium atoms [15] and $Z_3$ symmetry was also proposed as a way to solve baryon number violation in

[(a)]E-mail: mmd@if.ufrj.br

grand unified theories [16].

**Theoretical concept.** –  The magnetic field of the dipole $\boldsymbol{B} = [3(\boldsymbol{\mu}\cdot\hat{r}) - \boldsymbol{\mu}]/r^3$ produces a mixed state whose size can be estimated by simple arguments. Take its magnetic field, at the equatorial plane ($\boldsymbol{\mu}\cdot\hat{r} = 0$), and compare it to the known upper and lower critical field expressions obtained for a lattice of parallel flux lines, namely, $H_{c2} = \Phi_0/2\pi\xi^2$, and $H_{c1} = H_{c2}\ln\kappa/2\kappa^2$, respectively, where $\xi$ is the coherence length and $\kappa$ is the Ginzburg-Landau constant. The critical field regions are reached at distances $r(H_{c2}) = (\mu/\mu_0)^{1/3}\xi$ and $r(H_{c1}) = r(H_{c2})(2\kappa^2/\ln\kappa)^{1/3}$, respectively. The condition $r(H_{c2}) \geq \xi$ holds for a magnetic moment larger than $\mu_0 = \Phi_0\xi/2\pi$. In this case the volume around the magnetic moment, where superconductivity is destroyed has a radius larger than the minimal length scale $\xi$, the Cooper-pair size. The feasibility of such a magnetic domain with moment $\mu_0$ is verified by considering a finite volume instead of a point-like magnetic moment. Let us assume a spherically magnetized core with radius $r_M$, and compare its magnetization $M$ to the saturation magnetization, defined here to be one Bohr magneton per atom, $M_0 = \mu_B/(4\pi a_0^3/3) = 1.49$ tesla, where $a_0 \approx 0.05$ nm is the atomic radius. The Bohr magneton is $\mu_B = \Phi_0 r_c/2\pi$, and $r_c$ is the electron classical radius. For instance, for $\xi \approx 3.0$ nm, $\mu_0$ has nearly a million oriented Bohr magnetons ($\xi/r_c \approx 10^6$, $\xi/a_0 \approx 60$). In this case the magnetized core must have radius slightly larger than the coherence length, namely, $r_M \geq 1.7\xi$ in order to have a magnetization smaller than the saturation value ($M \leq M_0$). Here, we consider a type II superconductor of finite size, such that the London penetration length is much larger than the sample and therefore, $r(H_{c1})$ is never reached. The magnetic field streamlines around the magnetic moment are described in spherical coordinates by $r = a\sin^2\theta$, $a$ being a parameter associated to the loop size, and $\theta$ the angle with respect to the magnetic moment axis. This is a special case of the so-called rose curve, firstly described by the seventeenth century Italian mathematician, Guido Grandi.

To investigate the superconducting state of a sample with volume $V$, we minimize with respect to the order parameter $\psi$ the Ginzburg-Landau (GL) free energy

$$F = \int \frac{dv}{V}\left(|(-i\nabla - \frac{\boldsymbol{\mu}\times\boldsymbol{r}}{|\boldsymbol{r}|^3})\psi|^2 - |\psi|^2 + \frac{1}{2}|\psi|^4\right), \quad (1)$$

expressed in units of the critical field energy density, $F_0 = H_c^2/4\pi$. Note that in Eq. (1) all distances are scaled to $\xi$, and magnetic moment $\mu$ is given in units of $\mu_0$. The order parameter is kept equal to zero in the center of the sphere where the magnetic moment is located, a condition that does not affect our results since the previously described $H_{c2}$ normal core has radius larger than $\xi$ around the dipole. Three different and independent numerical methods were applied to this GL theory: simulated annealing minimization [17], integration of the GL equations [9], and kinetic energy eigenfunction expansion [18].
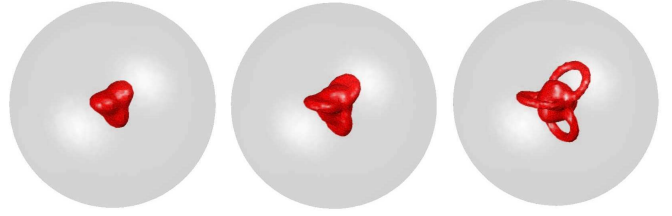


Fig. 1: (Colour on line) Isoplots of the Cooper-pair density for a magnetic moment $\mu/\mu_0$ equal to 15, 20, and 25 (left to right) in a superconducting sphere of radius $15.0\xi$. Red and grey surfaces are parts of the same isosurface drawn at 20 % of the maximum $|\psi|^2$.

Therefore, the present results were checked to be method independent. In what follows, we consider a sphere with radius $R = 15.0\xi$, and determine the vortex state as the magnetic moment $\mu$ is increased.

**The threefold symmetry.** –  As the magnetic dipole strongly suppresses superconductivity inside the $H_{c2}$ core, *vortex loops* nucleate as 3D objects in its vicinity, as shown in fig. 1. The following animations show a three-dimensional view of the loop states upon rotation of the sphere for the $\mu/\mu_0$ equal to 19 and 28 states, which correspond to embryonic and fully developed loop states, respectively: M19.mov and M28.mov (see multi_media file for more details about the animations). Distinctively from 2D vortices the length of the vortex line plays a fundamental role here. We find the remarkable result - a single loop or a pair of loops is not a stable state; three vortex loops are energetically favorable. With increasing dipole strength *vortex loops nucleate in triplets* from the $H_{c2}$ core, in a continuous manner, i.e. through a second order transition. We should emphasize that such a behavior was found regardless of the sample size (for $R > 10\xi$) and symmetry (e.g. sphere, cube), and is therefore a feature that holds also for bulk samples. The threefold growth of vortex loops is a consequence of the delicate energetic balance among the three-dimensional curved vortex lines. We used two methods to check its stability.

The first method is the kinetic energy eigenfunction expansion [18], a very appropriate method to prove this because near to the core the order parameter must be small. We expanded the order parameter, $\Psi = \sum_{k=1}^{\Omega} C_k\psi_k$ in the orthonormal eigenfunctions of the 3D kinetic energy operator $(i\hbar\nabla_{3D} - e^*\mathbf{A}/c)^2 \psi_k/2m^* = \epsilon_k\psi_k$. In cylindrically symmetric structures, these eigenfunctions have the form $\psi_{k=(L,n)} = \exp(iL\phi)f_n(r,\theta)$, where $L$ is the angular momentum, $\phi$ is the azimuthal angle around the dipole axis, and the index $n$ counts different states with the same $L$. The eigenfunctions $f_n$ are real and their corresponding eigenvalues are obtained numerically for each $L$, using the Housholder technique. Neumann boundary condition are assumed on the surface of the sample. The typical number of considered eigenfunctions is $\Omega$=10-50, with $L \in (-5, 5)$ and $n \in (1, 5)$. To search for the free energy minimum
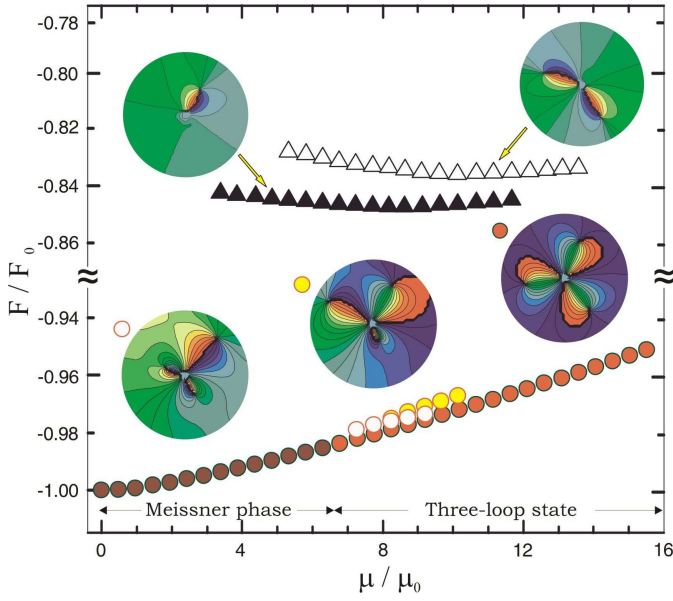
Fig. 2: (Colour on line) The free energy as a function of the dipole moment, obtained by the eigenfunction expansion method. Insets show the phase plots (blue/red - $0/2\pi$) of the corresponding vortex states, taken in the central cross-section perpendicular to the dipole.
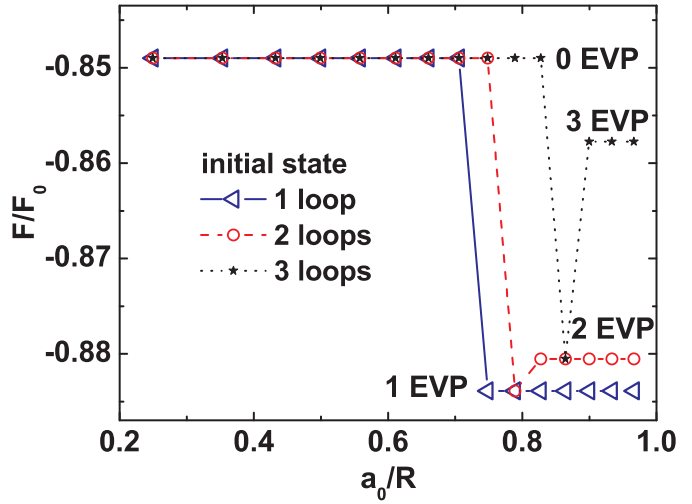


Fig. 3: (Colour on line) The free energy (arbitrary units) of the final relaxed state is shown versus the ratio loop size to radius, $a_0/R$, for the initial state. The magnetic moment is equal to $\mu/\mu_0 = 25$ and the initial states are made up of either one, two or three symmetrically arranged loops. If the initial state is near to the edge, the onset of *external vortex pairs* becomes possible otherwise not.

we map the superconducting state into a 2D cluster of $\Omega$ classical particles $(x_k, y_k) = (\Re(C_k), \Im(C_k))$, which is governed by the energy functional obtained when the expression for $\Psi$ is substituted in Eq. (1). In other words, the energy minimization with respect to the complex variables $C_k$ leads to the stable vortex states. Note that the total angular momentum of the vortex loops equals zero, thus both eigenfunctions with positive and negative $L$ must be included $[L \in (-L_{max}, L_{max})]$. Maximal considered vorticity $L_{max}$ determines the maximal achievable number of vortex loops. For $L_{max} = 1$ and $L_{max} = 2$, we were able to stabilize one and two loops respectively, but their energy was always significantly higher than the Meissner state, as shown in fig. 2. The encircling discontinuity of $2\pi$ (blue to red/red to blue) in the phase contour plots of fig. 2 signals a vortex/antivortex. However, when eigenfunctions with higher angular momenta were included in the calculation, the energy minima associated with just one and two loops ceased to exist. Instead, stable states with one pronounced loop and two 'satellite' ones (and vice versa) were found, yet with higher energy than the state with perfect threefold symmetry.

The second method used to support the stability of the three loop state is based on the minimization of the Ginzburg-Landau free energy through the simulated annealing procedure [17] starting from an initial constructed state, $\Psi_N(a, \phi)$, which depends on the following variables: the loop size, $a$, the azimuthal angle around the dipole axis, $\phi$, and the number of zeros of this wave function, $N$. This initial state is built such that the condition $\Psi_N(a_0, \phi_0) = 0$ holds for a single loop position, $a = a_0$,

and for a special azimuthal configuration determined by the condition $\exp(iN\phi_0) = 1$. Hence this initial state vanishes along $N$ symmetric loops. Obviously the above requirements don't uniquely define $\Psi_N(a, \phi)$, but we don't discuss the specific wavefunction taken here as we found invariance in our results with respect to this choice. For a fixed value of $\mu$ the numerical search for the minimum is carried and the final state free energy is shown in fig. 3 versus the initial loop size, $a_0/R$. Three distinct initial states were taken, i.e, $N = 1$, 2 and 3 CVLs. Indeed the numerical procedure yielded just one single final state with 3 CVLs regardless of the number of CVLs in the initial state, thus proving its stability. However this holds only for a small $a_0/R$ ratio, according to fig. 3. For a large $a_0/R$ ratio several final states are reached. The proximity to the boundaries explains this puzzling fact that for $a_0/R > 0.73$ the free energy minimum depends on the initial state, as shown in fig. 3. The proximity of $N$ loops to the surface of the sphere causes the onset of EVPs during the annealing procedure. In fact for the three highest values of $a_0/R$, the number of EVPs is exactly the number of CVLs in the initial state ($N$). This striking correlation leaves no doubt that an initial state with a CVL very near to the edge most easily turns into an EVP during the minimization procedure. Regardless of the number of EVP all the observed final vortex states of fig. 3 display three embryonic confined loops very near to the $H_{c2}$ core, as shown in fig. 4. The stability of states with other than three loops is only possible by explicitly breaking the azimuthal symmetry, such as in case of a rigid lattice of magnetic moments inside a bulk superconductor [19, 20].

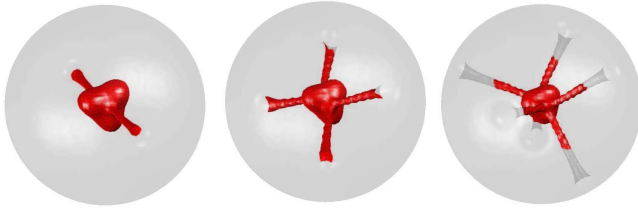Thus for a small superconducting sphere, i.e., with a ra-

Fig. 4: (Colour on line) Isoplots of the Cooper-pair density for three $\mu/\mu_0 = 25$ accessible states, namely, 1, 2 and 3 *external vortex pairs* (left to right) in a superconducting sphere of radius $15.0\xi$. Red and grey surfaces are parts of the same isosurface drawn at 20 % of the maximum.

tio $R/\xi$ not very large, the presence of boundaries strongly influences the vortex state as seen in figs. 3 and 4. This is because CVLs very near to the superconductor's external surface eventually break and spring to the surface in the form of EVPs. Next we discuss some general aspects of these states. The switch of a CVL into an EVP induces a first order transition. EVPs are shown in fig. 4 in a grey and red color scheme. Red and grey colors describe parts of a single isosurface contained in distinct concentric volumes. Inside a inner cubic cell the isosurface is red and in the remaining volume grey. Thus a CVL is always red, whereas the EVPs are double colored, red and grey. The external isosurface, including the regions of contact with the EVPs are represented in grey color. Thus for the finite size superconductor the vortex state is generally classified according to the number of CVLs and of EVPs, an important difference to previous 2D studies [12–14] where the only distinction is between 'giant' and 'multi' vortex states. States with multiple EVPs manifest as a collection of vortices on the sample surface, but are conjoined to a giant vortex in the sample center. The total angular momentum ('winding number', or 'vorticity') increases by one for each additional EVP. According to fig. 4 this giant vortex also contains three embryonic CVLs. The following animations show three-dimensional views of some $\mu/\mu_0$ states, namely, for 24, 34, and 31. These states show 3 embryonic CVLs with 1, 2 and 3 EVPs, respectively: M24.mov, M34.mov and M31.mov (see multi_media.doc file for more details about the animations). The CVL to EVP (first order) transitions lead to jumps in the magnetization ($M = -\partial F/\partial\mu$), shown in fig. 5 as a function of the dipole moment $\mu$. Note that this feature directly leads to accessible experimental detection of EVP states, e.g. by Hall-probe magnetization measurements. However, the observation of CVL states is more demanding and requires a combination of various complementary microscopic experimental techniques, such as Small Angle Neutron Scattering (SANS), muon spin rotation ($\mu$SR) [21], and possibly scanning tunneling microscopy on curved surfaces to detect the threefold slight suppression of the order parameter on the surface of the sphere [as shown in grey scale of figs. 5(a-c)].
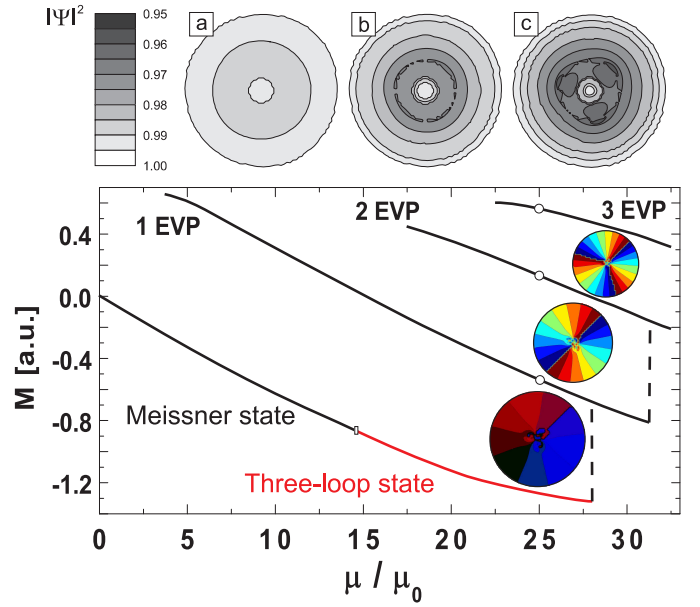


Fig. 5: (Colour on line) Sample magnetization (in arbitrary units) vs. dipole moment. Insets show the phase in the equatorial plane of the sample for the 1-3 *external vortex pair* states of fig. 4 (for $\mu/\mu_0 = 25$, open dots). (a)-(c) $|\psi|^2$ contourplots of the top half hemisphere of the sample, for the three *confined vortex loops* state and $\mu/\mu_0 = 20$, 24, and 28, respectively.

**The evolution of the vortex state.** – The onset of EVPs unveils interesting aspects of the threefold symmetry because of the soft breaking interactions that drive such first order transitions. A CVL becomes unstable near to the surface of the superconductor and eventually breaks apart giving rise to a EVP, as shown in figs. 2-5. For our spherical sample the three initially equivalent loops are naively expected to grow and reach the surface simultaneously, turning into three EVPs. Nevertheless one and two EVPs are also observed implying that the threefold symmetry is disturbed during its evolution by some soft breaking mechanism, here caused by the use of a cubic grid. The evolution of the remaining two CVL, as the third one turns into an EVP, is quite remarkable. The outgrowth of one particular CVL from the threefold state causes: (i) the shrinkage of the other two ones and (ii) the appearance of a new CVL to recover the threefold symmetry near the $H_{c2}$ core. This shows that it is easier to recover the threefold symmetry near the $H_{c2}$ core because there the CVLs are less energetically costly to produce. The development of the symmetry during the simulated annealing transition from 0 to 1 EVP is shown in fig. 6. A 3 CVL state becomes unstable at $\mu/\mu_0 = 28.5$ [fig. 6(a)] and evolves, under controlled annealing temperature, to a 1 EVP state. Threefold symmetry is observed *both below and above* the transition point. A trapped intermediate (unstable) configuration during this transition is shown as inset (b) of fig. 6. We confirmed these results by a saddle-point analysis [18], carried through the kinetic energy eigenfunction expansion. Moreover we have shown
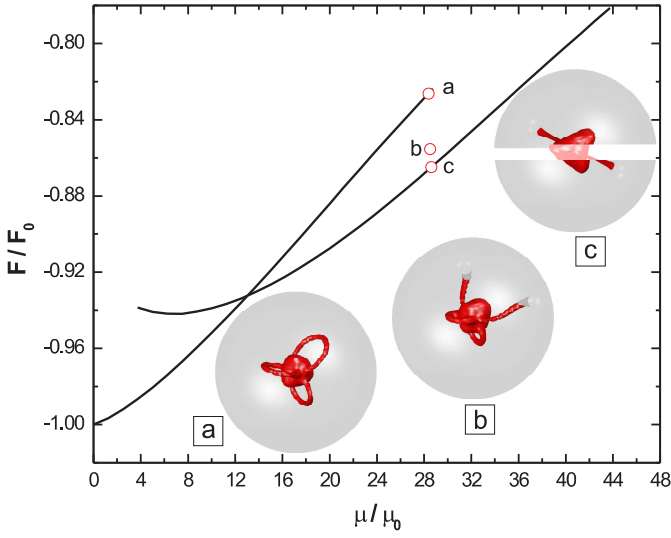
Fig. 6: (Colour on line) The free energy curves versus dipole moment for 0 and 1 *external vortex pair* state obtained by the simulated annealing method. The *confined vortex loop* state is metastable for $\mu/\mu_0 > 12.5$ and becomes unstable at $\mu/\mu_0 = 28.5$. The isosurfaces in the insets (a-c) show snapshots of the consequent 0 to 1 *external vortex pair* transition.

that the presence of an external current applied along the magnetic dipole can induce this transition, as shown in the following animation done for $\mu/\mu_0 = 10$: ZERO-TO-ONE.mov (see multi_media file for more details about the animations). The density increases away from the $H_{c2}$ core at the center but eventually this growth stops and the trend reverts to a decreasing pattern near to the surface of the mesoscopic sphere. Outside the order parameter must rigorously vanish, and so, there is always an external isosurface density near to the surface of the mesoscopic sphere with constant and small $|\psi|^2$. The figs. 1, 4 and 6 show it in grey scale as part of the isosurface drawn at 20 % of the maximum $|\psi|^2$.

Conclusion. – Using several independent theoretical approaches, we found a *threefold* embryonic growth of vortex loops from the $H_{c2}$ core surrounding the magnetic moment in a superconducting sphere. As shown here, the superconducting state with three vortex loops is energetically favorable over one or two vortex loops regardless of the sample boundaries. Therefore, our results also apply to bulk samples. We expect that the present scenario of loop breaking at the sample surface can be useful to understand properties of a bulk superconductor with some distribution of magnetic domains in its interior, where growing vortex loops may interconnect neighboring magnets rather than spring to the surface, which would lead to the experimentally observable spontaneous vortex phase [22]. The puzzling properties of the recently discovered ferromagnetic superconductors [23] and superconducting ferromagnets [24, 25] are indicative of vortices stemming from an internal magnetic field. We expect that the recent ad-vancements in material synthesis, which have led to several fabricated nano-composites, such as the $MgB_2$ superconductor with embedded magnetic $Fe_2O_3$ nanoparticles [26], or Gd particles incorporated in a Nb matrix [27], can be used to obtain the predicted vortex patterns made of confined vortex loops and external vortex pairs.

∗ ∗ ∗

REFERENCES

[1] NEMIROVSKII S. K. and FISZDON W., *Rev. Mod. Phys.*, **67** (1995) 37.
[2] NABARRO F. R. N., *Theory of Crystal Dislocation*, (Oxford University Press, Oxford) 1967.
[3] COPELAND E. J., KIBBLE T. W. B. and STEER D. A., *Phys. Rev. D*, **58** (1998) 043508.
[4] MAGUEIJOA J., SANDVIK H. and STEER D. A., *Phys. Rev. D*, **60** (1999) 103514.
[5] WIEGEL F. W., *Introduction to Path-Integral Methods in Physics and Polymer Science*, (World Scientific Publishing, Singapore) 1986.
[6] ABRIKOSOV A., *Sov. Phys. JETP*, **5** (1957) 1174.
[7] KLEINER W. H., ROTH L. M. and AUTLER S. H., *Phys. Rev. A*, **133** (1964) 1226.
[8] GEIM A. K., GRIGORIEVA I. V.,DUBONOS S. V. ,LOK J. G. S., MAAN J. C., FILIPPOV A. E. and PEETERS F. M., *Nature (London)*, **390** (1997) 259.
[9] SCHWEIGERT V. A., PEETERS F. M. and DEO P. S., *Phys. Rev. Lett.*, **81** (1998) 2783.
[10] KANDA A., BAELUS B. J., PEETERS F. M., KADOWAKI K. and OOTUKA Y., *Phys. Rev. Lett.*, **93** (2004) 257002.
[11] BAELUS B. J. and PEETERS F. M., *Phys. Rev. B*, **65** (2002) 104515.
[12] MILOŠEVIĆ M. V. and PEETERS F.M., *Phys. Rev. B*, **68** (2003) 024509.
[13] MILOŠEVIĆ M. V. and PEETERS F.M., *Phys. Rev. Lett.*, **93** (2004) 267006.
[14] MILOŠEVIĆ M. V. and PEETERS F.M., *Phys. Rev. Lett.*, **94** (2005) 227001.
[15] KRAEMER T., MARK M., WALDBURGER P., DANZI J. G., CHIN C., ENGESER B., LANGE A. D., PILCH K., JAAKKOLA A., NAGERL H. C. and GRIMM R., *Nature (London)*, **440** (2006) 315.
[16] AGASHE K. and SERVANT G., *Phys. Rev. Lett.*, **93** (2004) 231805.
[17] DORIA M. M., GUBERNATIS J. E. and RAINER D., *Phys. Rev. B*, **41** (6335) 1990.
[18] SCHWEIGERT V. A. and PEETERS F. M., *Phys. Rev. Lett.*, **83** (1999) 2409.

[19] DORIA M. M., *Physica C*, **404** (2004) 145.

[20] DORIA M. M., *Physica C*, **408** (2004) 466.

[21] SONIER J. E. , KIEFL R. F., BREWER J. H., CHAKHALIAN J., DUNSIGER S. R., MACFARLANE W. A., MILLER R. I., WONG A., LUKE G. M. and BRILL J. W., *Phys. Rev. Lett.*, **79** (1997) 1742.

[22] NG, T. K. and VARMA, C. M., *Phys. Rev. Lett.*, **78** (1997) 330.

[23] BLUHM H., SEBASTIAN S. E., GUIKEMA J. W., FISHER I. R. and MOLER K. A., *Phys. Rev. B*, **73** (2006) 14514.

[24] SAKAI H., OSAWA N., YOSHIMURA K., FANG M. and KO-SUGE K., *Phys. Rev. B*, **67** (2003) 184409.

[25] JORGENSEN J. D., CHMAISSEM O., SHAKED H., SHORT S., KLAMUT P. W., DABROWSKI B. and TALLON J. L., *Phys. Rev. B*, **63** (2001) 54440.

[26] SNEZHKO A., PROZOROV T. and R. PROZOROV, *Phys. Rev. B*, **71** (2005) 024527.

[27] PALAU A., PARVANEH H., STELMASHENKO N. A., WANG H., MACMANUS-DRISCOLL J. L. and BLAMIRE M.G., *Phys. Rev. Lett.*, **98** (2007) 117003.

# Threefold onset of vortex loops in superconductors with a magnetic core

Mauro M. Doria[1,2] [(a)] and Antonio R. de C. Romaguera[1,2] and M. V. Milošević[1,3] and F. M. Peeters[1]

[1] *Departement Fysica, Universiteit Antwerpen, Groenenborgerlaan 171, B-2020 Antwerpen, Belgium*
[2] *Instituto de Física, Universidade Federal do Rio de Janeiro, C.P. 68528, 21941-972, Rio de Janeiro RJ, Brazil*
[3] *Department of Physics, University of Bath, Claverton Down, BA2 7AY Bath, United Kingdom*

PACS 74.25.Ha – Magnetic properties
PACS 74.25.Op – Mixed state, critical fields, and surface sheath
PACS 74.78.Na – Mesoscopic and nanoscale systems

**Abstract.** - A magnetic inclusion inside a superconductor gives rise to a fascinating complex of *vortex loops*. Our calculations, done in the framework of the Ginzburg-Landau theory, reveal that *loops always nucleate in triplets* around the magnetic core. In a mesoscopic superconducting sphere, the final superconducting state is characterized by those confined vortex loops and the ones that eventually spring to the surface of the sphere, evolving into *vortex pairs* piercing through the sample surface.

Examples of one- or multi-dimensional collections of topological defects arise in various physical systems, such as vortices in quantum fluids [?], dislocations in solids [?], global cosmic strings [?, ?], and polymer chains [?]. Changes of symmetry in their structural and dynamical properties often lead to very rich phase transitions. In superconductivity, the structure and symmetry of the vortex lines has been a major issue even in the early days, when Abrikosov [?] proposed a square pattern for the lattice of penetrating flux tubes in bulk superconductors; later on, Kleiner *et al.* [?] found that the most efficient way to pack interacting parallel rods is actually through a hexagonal pattern. However, in systems with reduced dimensionality, the Abrikosov symmetry of the vortex state can be strongly affected by the sample boundaries. In mesoscopic superconductors, where the volume to surface area ratio is small [?], strong lateral confinement may impose the formation of multiquanta ('giant') vortices [?, ?], while the shape of the boundary directs the symmetry of the final vortex configuration [?].

In this Letter, we consider a novel vortex structure that stems from the specific *inhomogeneous* magnetic field of a point like magnetic dipole with moment $\mu$ in the center of a superconducting sphere. This magnet is the only source and sinkhole of vortex lines and sets an axis around which the vortex state exhibits a discrete symmetry. Because

the sphere does not break this degeneracy many of the present results also apply for a magnetic inclusion in a bulk superconductor.

Therefore, the present analysis is very different from earlier studies of vortex and antivortex structures in superconductor/magnet hybrids [?,?,?] where magnetic dots were placed near, but *outside* a *thin* superconducting sample. While in the latter case vortices were two-dimensional (2D) structures characterized by a coin-like core, here they are lines in three-dimensional (3D) space, set on a formalism that comprises the full 3D Ginzburg-Landau theory, thus far more complex than previous works. Consequently, novel vortex phases with profound 3D features are found for these sets of curved vortex lines, made of *confined vortex loops* (**CVL**s) and *external vortex pairs* (**EVP**s).

For small $\mu$, as shown later, we find that the vortex state is made of *exactly three* confined vortex loops around the dipole axis. For an increasing magnetic moment $\mu$ more elaborate vortex arrangements arise because of the inhomogeneity of the field. This threefold growth of vortex loops in our system is shown here to be a consequence of the energetic balance. Threefold symmetry has been a source of inspiration since the sixties when its discovery in hadronic physics has led to quarks as the basic constituents of matter. Recently, experimental evidence was found for the onset of trimer bound states in ultracold gases of caesium atoms [?] and $Z_3$ symmetry was also proposed as a way to solve baryon number violation in grand

[(a)]E-mail: mmd@if.ufrj.br